Characterization of (La1-xSrx)(s)MnO3 and Doped Ceria Composite Electrodes in NOx-Containing Atmosphere with Impedance Spectroscopy

Werchmeister, Rebecka Maria Larsen; Kammer Hansen, Kent; Mogensen, Mogens Bjerg

Published in:
Journal of The Electrochemical Society

Link to article, DOI:
10.1149/1.3327892

Publication date:
2010

Document Version
Publisher's PDF, also known as Version of record

Journal of The Electrochemical Society, **157** (5) P35-P42 (2010)
0013-4651/2010/157(5)/P35/8/$28.00 © The Electrochemical Society

Characterization of $(La_{1-x}Sr_x)_sMnO_3$ and Doped Ceria Composite Electrodes in NO_x-Containing Atmosphere with Impedance Spectroscopy

R. M. L. Werchmeister,[z] K. Kammer Hansen,[*] and M. Mogensen[*]

Fuel Cells and Solid State Chemistry Division, Risø National Laboratory for Sustainable Energy, Technical University of Denmark, DK-4000 Roskilde, Denmark

This study used electrochemical impedance spectroscopy (EIS) to characterize composite metal oxide electrodes in atmospheres containing NO, NO_2, and O_2. Symmetrical cells with electrodes of $(La_{1-x}Sr_x)_sMnO_3$ [$(x,\ s)$ = (0.15, 0.9) and (0.5, 0.99)] and doped ceria [$Ce_{0.9}Gd_{0.1}O_2$ and $Ce_{1-x}Gd_xO_2$ (x = 0.1, 0.2)] were subjected to EIS while varying the temperature (from 300 to 600°C), the composition of the atmosphere, and the gas flow. The impedance spectra were fitted to equivalent circuits, and common arcs were identified and sought related to physical and chemical processes. The electrodes had a much lower polarization resistance (R_p) when NO or NO_2 was present in the atmosphere at low temperatures (300–400°C) than in air. The impedance spectra for electrodes in 1% NO in Ar were dominated by a low frequency arc at high temperatures (500–600°C). This arc seemed to be a type of conversion arc, which is related to a gaseous intermediate (possibly NO_2), formed from NO, through which the electrode reaction occurs. Indications were found that the electrodes are not electrochemically active toward NO around open-circuit voltages.
 [DOI: 10.1149/1.3327892]

Manuscript submitted October 21, 2009; revised manuscript received December 7, 2009. Published March 15, 2010.

Nitrogen oxides are formed from O_2 and N_2 at the high temperatures found in combustion engines. NO_x is poisonous for human beings and is a threat to the environment. Therefore, great focus is on detecting and removing NO_x. NO_x can be reduced electrochemically, as first shown in Ref. 1, and since then several studies have been done concerning the electrochemical removal of NO_x.[2-4] Electrochemical removal of NO_x has been suggested as a method to remove NO_x from the exhaust stream of a diesel engine where oxygen is present.[5] NO reduction after removing O_2 by electrochemical pumping was demonstrated by Hibino et al.[6]

A solid oxide electrochemical cell with composite oxide electrodes can be used to remove NO_x. The idea is that NO_x is reduced at the cathode (Eq. 1), resulting in the formation of N_2, while the oxygen ions are transported through the electrolyte to the anode, where O_2 is formed (Eq. 2)

$$\text{Cathode} \quad NO + 2e^- \rightarrow \tfrac{1}{2}N_2 + O^{2-} \qquad [1]$$

$$\text{Anode} \quad O^{2-} \rightarrow \tfrac{1}{2}O_2 + 2e^- \qquad [2]$$

The oxygen reduction reaction (Eq. 3) is a competing reaction, which can also take place at the cathode

$$\text{Cathode} \quad O_2 + 4e^- \rightarrow 2O^{2-} \qquad [3]$$

This work is part of a technological explorative investigation of the $(A_{1-x}A'_x)_{1-\delta}B_{1-y}B'_yO_3$–$M^h_{1-z}M^d_zO_2$ perovskite electrode system with respect to possibilities of finding combinations that might work as NO reduction electrodes. A and A′ are large A-site ions in the ABO_3-type perovskite; M^h and M^d are the metal host ion and dopant ion in the MO_2-type fluorite. Two sets of relatively different materials within the same family were studied, $(La_{0.5}Sr_{0.5})_{0.99}MnO_3$ (LSM50) and $Ce_{1-x}Pr_xO_2$ (CPO) (x = 0.1, 0.2) and $(La_{0.85}Sr_{0.15})_{0.9}MnO_3$ (LSM15) and $Ce_{0.9}Gd_{0.1}O_2$ (CGO). Both LSM15 and LSM50 are A-site substoichiometric resulting in extra MnO_x, but LSM15 has 10 times more than LSM50. Thus, this testing of different sets of composite electrodes, which have potential for activity toward the electrochemical removal of NO, is a kind of digging down into different sites in a corner of the vast field of the ABO_3–MO_2 composite electrodes. It was decided to investigate the composite electrodes of $La_{1-x}Sr_xMnO_3$ (LSM) and CGO or CPO. These materials were chosen because various perovskites have been tested for activity toward the decomposition of NO_x [7-9] and electrochemical reduction,[4] and among them LSM showed activity. CPO can conduct both electrons and oxide ions, and the praseodymium ions in CPO can easily change oxidation state between 3+ and 4+, which might provide some catalytic activity for the reduction reaction.

In the field of electrochemical removal of NO_x, Reinhardt et al.[2] used electrochemical impedance spectroscopy (EIS) on tip electrodes to determine the number of time constants, i.e., the number of limiting processes. EIS has also been used for the characterization of electrochemical cells for NO_x detectors.[10,11] Further, ac measurements on symmetric electrochemical cells have been used earlier in cells for NO_x detection.[12,13] EIS has been used intensively to characterize electrodes and to obtain knowledge about kinetics in the field of solid oxide fuel cells (SOFCs). Separation of the arcs that compose the impedance spectra can give valuable information about how adsorption takes place, electrode structure, and current transfer.

Symmetrical cells in a one atmosphere setup were used for the characterization; the gas composition was not monitored. The EIS measurements were done in the temperature range of 300–600°C. The range of 300–400°C corresponds well with the temperature in the actual exhaust of a diesel engine. Information about the temperature dependence can be found by measuring over a broader temperature range, so the temperature range was expanded to 600°C. Also, at 600°C, it is possible to compare results for measurements in air with existing results, as this is in the low temperature end of SOFCs temperature operating range.

Experimental

The electrochemical experiments were carried out using a symmetrical cell, which is a two-electrode cell where the electrodes on both sides of the cell are identical.

The powders of LSM50, $Ce_{0.9}Pr_{0.1}O_2$ (CPO10), and $Ce_{0.8}Pr_{0.2}O_2$ (CPO20) were synthesized by the glycine nitrate combustion synthesis,[14] and the LSM50 powder was made with 1% Mn in excess. The Mn, La, Pr, and Sr nitrates were from Alfa Aesar, and the Ce nitrate was from Johnson Matthey. The CPO powders were calcined at 1000°C for 6 h, while the LSM50 powder was calcined at 1200°C for 50 h. X-ray powder diffraction with a theta–theta STOE diffractometer was used to determine if the powders were single phased.

The $Ce_{0.9}Gd_{0.1}O_2$ (CGO10) powder was a commercial product from Rhodia, and the LSM15 powder was from Haldor Topsoe A/S.

A sintered tape of CGO10 with a thickness of around 160 μm was used as an electrolyte. A slurry with CGO powder and binder

* Electrochemical Society Active Member.
[z] E-mail: rewe@risoe.dtu.dk

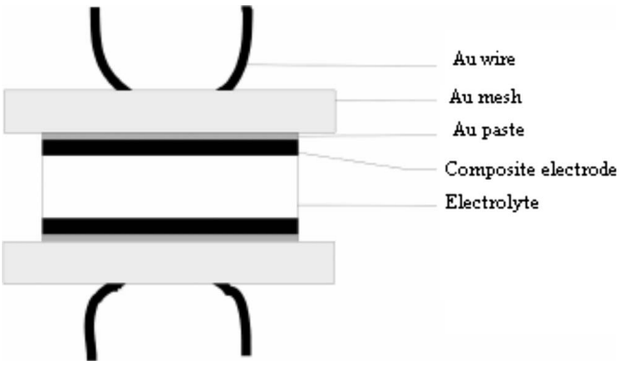

Figure 1. A sketch of the symmetrical cell setup.

was tape casted, and the tape was subsequently sintered at 1150°C. The electrodes were screen printed on both sides of the 50 × 50 mm CGO10 tape, and the cells were sintered at 1050°C for 2 h.

Terpineol-based screen printing pastes were made by mixing the powders with a solvent, milling on a planetary mill, and finally adding a binder. The particle size distribution was measured with a Beckman Coulter particle size analyzer, and the pastes were milled until a d_{90} value below 7 μm was obtained for all of them.

Afterward, the big cells (50 × 50 mm) were cut into small cells of approximately 6 × 6 mm with a diamond tool.

Three different electrodes were prepared: one with 50 wt % LSM15 and 50 wt % CGO10 (LSM15/CGO10), another with 50 wt % LSM50 and 50 wt % CPO10 (LSM50/CPO10), and the last with 50 wt % LSM50 and 50 wt % CPO20 (LSM50/CPO20).

The electrodes of the symmetrical cells were examined with focused ion beam–scanning electron microscopy (FIB–SEM) to view the microstructure. The sample was prepared by mounting in a Cold Mount resin supplied by Structure Probe Inc. at atmospheric pressure. A Zeiss XB 1540 CrossBeam was used for both SEM imaging and FIB milling. The accelerating voltage was 10 kV, and the SE2 detector of the XB 1540 was used. Furthermore, the polished cross section of the cells mounted in epoxy was examined in a Hitachi tabletop microscope (TM1000).

Gold paste with 20 wt % carbon was painted on the sides of the symmetrical cell as a current collector. The carbon was added as a pore former.

The symmetrical cells were placed in a setup, as shown in Fig. 1. Gold wires and a gold net were used as current collectors. Platinum cannot be used because it is catalytically active in the decomposition of nitrogen oxide.

Four small cells with similar electrodes were placed in an oven with a controlled atmosphere. The setup was heated to 850°C to remove the carbon in the gold paste and to make the gold paste come into contact with the gold net and the electrodes, and this was done in air.

Afterward, electrochemical measurements were done at 600, 500, 400, and 300°C in different atmospheres: air, 1% NO in Ar, 1% NO_2 in Ar, and 0.75% NO + 5% O_2 in Ar. Furthermore, the LSM50/CPO20 electrodes were subjected to EIS in 1% N_2O in Ar at 500 and 600°C. A gas flow of 100 mL/min was used unless anything else is stated.

The 350-S flue gas analyzer from Testo was used to measure the ratio between the concentration of NO and NO_2 at 400, 500, and 600°C in the outlet gas from the setup. The gas analyzer uses electrochemical sensors to detect NO and NO_2.

A Solartron 1260 frequency response analyzer was used for the EIS characterization of the cells. This was done at an open-circuit voltage (OCV) and with an amplitude of 36 mV root-mean-square over the cell and an internal resistor of 50 Ω. The maximum frequency was 1 MHz, and the lowest was 1–100 mHz.

EIS was used to test the electrodes. Electrochemical impedance measurements were done by applying an alternating voltage signal over the cell and then measuring the current response. The ac current response was phase shifted compared to the ac potential. The impedance was defined as the ratio between the potential and the current response. Only a small potential amplitude was used as the system response must be linear.

The impedance of the electrode reveals to which degree it is resisting the polarization. When the cell is polarized, current runs and the electrochemical processes can take place; i.e., the electrodes are active and surface reactions with NO_x can occur. So, the impedance can tell how hindered the electrodes' activity is. Usually, the impedance spectrum consists of several overlapping arcs, which can be separated by fitting equivalent circuits to the experimental data.

Ideally, the polarization impedance is composed of several resistances (R) with associated capacitances (C). These RC units connected in series make up the total impedance spectrum. The constant phase elements (CPEs) are used instead of capacitances because of the nonideal behavior of the system. The impedance for the CPE can be seen in Eq. 4[15]

$$Z = \frac{1}{Y_0(j\omega)^{\alpha}} \quad [4]$$

RQ elements replace RC, but the Q values are dependent on the frequency and cannot be directly compared to the capacitance. Therefore, the equivalent capacitance (EC), also called C_ω defined in Eq. 5, is used, which is the capacitance calculated from the summit frequency of the arc, as described in Ref. 16

$$C_\omega = R^{(1-\alpha)/\alpha} Q^{1/\alpha} \quad [5]$$

When the atmosphere is changed, the pO_2 changes. The LSM, CGO, and CPO electrodes desorp O_2 when the pO_2 is low, thereby changing the electrodes' properties. This should be taken into account when viewing the results for measurements in atmospheres with changing pO_2.

The data obtained were analyzed with "Equivalent circuit for Windows" from University of Twente.[17] The simplest possible fit with series-connected (RQ) elements was sought for. Then, the arcs found were compared, and some trends in α values (see Eq. 4) and ECs were recognized. Average α values were found for similar arcs, and the data were remodeled holding the α values constant. The EC and resistances obtained were assumed to represent real physical processes.

More than 180 impedance spectra were used for the analysis, varying the type of electrode, temperature, atmosphere, and flow rate.

Results

Microstructure.— The thickness of the electrodes was approximately 20 μm, and the structure was porous. The microscopy pictures showed mostly small particles of less than 1 μm diameters along with some larger particles of up to 5 μm diameters. The FIB was used to mill a trench in the cell and a picture of the cut can be seen in Fig. 2, where both the LSM50/CPO20 electrode and some of the dense CGO electrolyte are visible. The electrode appears to be slightly disconnected from the electrolyte. This is likely an artifact from the preparation of the sample for microscopy, but it still indicates that the contact between the electrodes can be improved.

Data treatment.— The difference between the high frequency (HF) and low frequency (LF) intercepts with the x-axis in the impedance spectra is the polarization resistance of the electrodes of the cell, $2R_p$, as shown in Fig. 3.

For the three types of composite electrodes, three to four arcs were identified in the impedance spectra depending on temperature, electrode composition, and atmosphere.

The following steps were used to treat the large amount of EIS data.

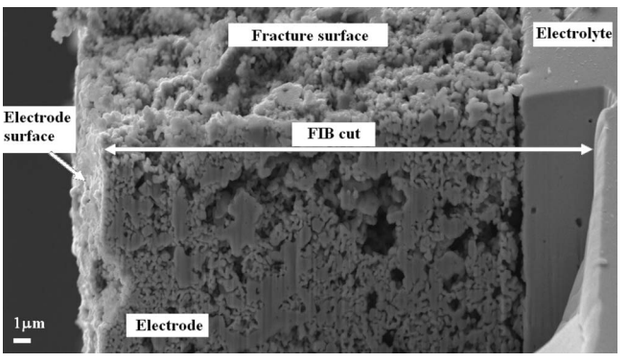

Figure 2. FIB–SEM image of the LSM50/CPO20 electrode and part of CGO electrolyte.

1. An equivalent circuit was fitted to every set of impedance spectra without any restrictions on values of parameters or number of arcs.
2. Then, the resulting equivalent circuits were compared. Arcs appearing in the multiple impedance spectra with similar capacitances and α values were identified.
3. For the identified arcs, average α values were calculated.
4. The data were fitted again, this time with the identified number of arcs with average α values locked.

To use this approach, it is important to have many impedance spectra, both for similar cells under identical conditions, but also varying parameters such as atmosphere, temperature, and flow rate. This is necessary because there are many free parameters in the fit, and more EIS data ensure a more realistic picture.

As an example, the impedance spectra for the LSM50/CPO10 electrodes in 1% NO in Ar at 600°C could be fitted with two to four arcs. It can be determined visually from the spectrum in Fig. 4 that at least two arcs are present: a large dominating LF arc and a smaller arc at higher frequencies. By enlarging the HF area (Fig. 5), it is seen that for the fit with two arcs, the middle frequency (MF) arc cannot fully model the HF data points. Adding another or two other arcs provides a better fit in the HF range, and the χ^2 value decreases from 2.5×10^{-3} to 2.1×10^{-4} and 1.6×10^{-4}. The fit with four

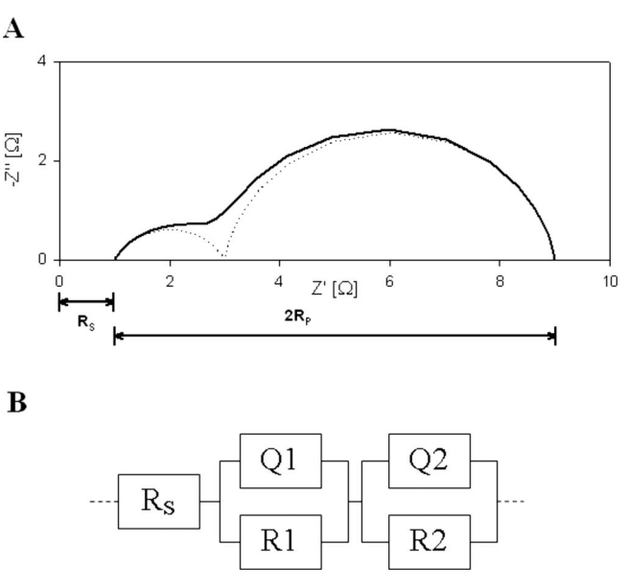

Figure 3. (A) Sketch of impedance plot of symmetrical cell with marked R_p and serial resistance, R_S. (B) Corresponding equivalent circuit.

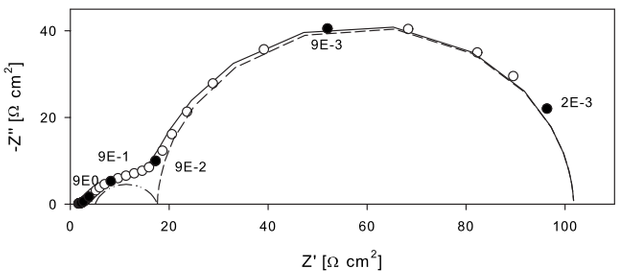

Figure 4. The impedance spectra for LSM50/CPO10 electrodes in 1% NO at 600°C along with the deconvolution of the data (dotted lines). For the solid points the frequency of the data point is given in hertz.

arcs only decreases the χ^2 25% extra compared to the fit with three arcs, and it is seen in Fig. 5 that the main part of the extra HF arc is located outside the experimental data range. Applying an extra arc nearly always improves the fit but does not necessarily have any physical meaning to the system. Also, adding extra unknown parameters to be fitted from the same amount of data increases the uncertainty, so the smallest number of arcs should be used to get a reasonable fit. Therefore, the fit with three arcs is assumed to be optimal. It is close to the experimental data both at HF and LF, and the decrease in χ^2 by adding another arc is very little.

The average α values for the LSM50/CPO electrodes were 1 for the LF arc, 0.7 for the MF arc, and 0.35 for the HF arc. The very low α value for the HF arc raises the question of whether it represents a real process or HF measurement errors. Fitting the spectra with the average α values did not change the χ^2 value, which indicates that the average α values are correct.

The next step is to repeat the approach for the sets of impedance spectra recorded at difference temperatures and for other types of electrodes and to compare the arcs identified. This may lead to sets of arcs with average α values, which can be used for all impedance spectra within a group. For instance, electrodes with LSM50 and CPO*X* (X = 10, 20) in 1% NO in Ar at 500–600°C can be fitted with the same set of arcs. The impedance plot for the LSM50/CPO10 cells in air at 600°C were composed of three arcs, as seen in Fig. 6. Some impedance spectra were better fitted with four arcs, such as the spectra for the LSM15/CGO10 electrodes in 1% NO_2 in Ar at 600°C (see Fig. 7). The data points measured at LF sometimes showed time dependence; i.e., the system was not stable over the time period that the measurement requires. Therefore, some of these points were disregarded in the fitting process.

The apparent activation energy was calculated from the slope of the logarithm of the inverse resistance as a function of the inverse

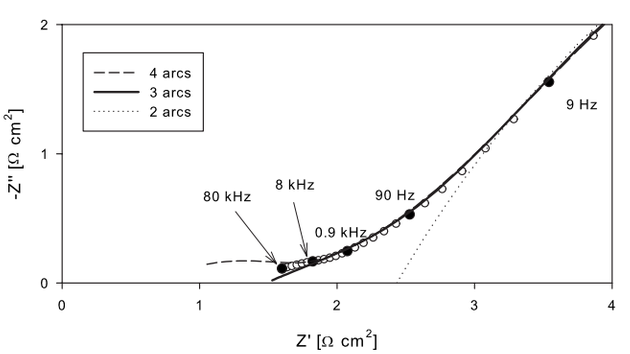

Figure 5. HF close up of impedance spectra of symmetrical cell with LSM50/CPO10 electrodes in 1% NO in Ar at 600°C along with the fit with two (⋯), three (—), and four (- - -) arcs.

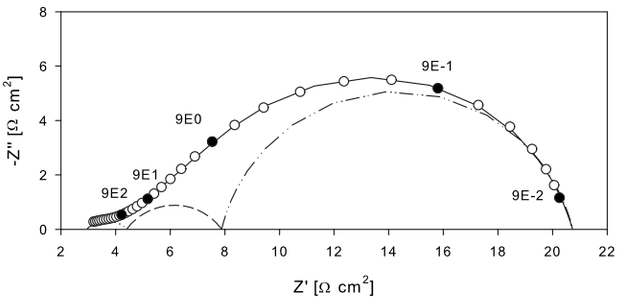

Figure 6. Impedance plot for LSM50/CPO10 electrodes in air at 600°C along with the deconvolution of the data (dotted lines). For the solid points, the frequency of the data point is given in hertz.

temperature. In some cases, the points were very close to linearity, while in other cases, the points form a curve, and there are probably two activation energies.

The overall apparent activation energy calculated for the total R_p for all the cell types can be seen in Table I. The apparent activation energy is the activation energy calculated from an approximate straight line disregarding the value of R^2, so in some cases, it is an

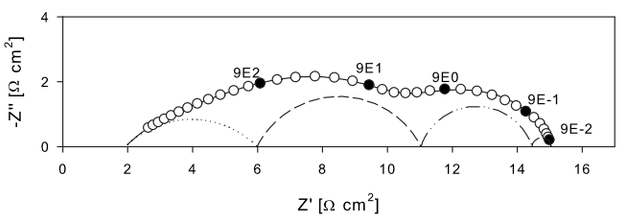

Figure 7. Impedance plot for LSM15/CGO10 electrodes in 1% NO_2 in Ar at 600°C along with the deconvolution of the data (dotted lines). For the solid points, the frequency of the data point is given in hertz.

average of two (or more) different activation energies. The total R_p can be used as a crude estimate of the activity of the electrodes in NO_x, although it consists of resistances from several different electrode reaction steps, which likely have different activation energies.

The standard deviation between the small cells are noted along with the square of the correlation coefficient value (R^2) for the linear regression.

Air.— In the impedance spectra for all types of cells in air, there was one large frequency arc and two to three smaller arcs at higher frequencies. The large arc had an EC in the range of 10^{-4}–10^{-2} F cm^{-2} depending on electrodes and temperature (see Fig. 6, for example). Typically, there were three to four arcs in the impedance spectra.

For the cells with LSM15/CGO10 electrodes, there were three arcs at 600°C and four arcs at the lower temperatures. The impedance plots for cells with electrodes of LSM50/CPO10 were also composed of three to four arcs, while only three arcs were found in the impedance spectra for cells with electrodes of LSM50/CPO20 in air.

NO.— When the cells were subjected to impedance spectroscopy in an atmosphere of 1% NO in Ar, three to four arcs were necessary to model the spectra. A large arc at very low frequencies dominated the spectra, followed by a smaller arc in the MF region and some smaller arcs in the HF end (see Fig. 4).

The EC of the LF arc increased with the content of Pr. The LF arc did not increase as much with decreasing temperature as the MF arc. As a result, the MF arc dominated at the lower temperatures, and at 300°C, the LF arc could not be separated from the spectra. The activation energy for the MF and LF arcs along with their EC for the three electrodes can be found in Table II. Figure 8 shows the resistance of the HF, MF, and LF arcs for LSM15/CGO10 electrodes.

The flow of gas was changed from 100 to 10 mL/min. This had a large effect on the LF arc in the NO spectra (see Fig. 9), and R_{LF}

Table I. The overall apparent activation energy for electrodes in air, 1% NO in Ar, 1% NO_2 in Ar, and 0.75% NO + 5% O_2 in Ar over the temperature range of 300–600°C in a flow of 100 mL/min together with the corresponding R^2 values for the fit and R_p values at 600°C.

		LSM15/CGO10	LSM50/CPO10	LSM50/CPO20
Air	E_a (eV)	0.88 ± 0.01	1.06 ± 0.06	1.11 ± 0.02
	R^2	0.972	0.978	0.965
	R_p (600°C) (Ω cm^2)	8.8 ± 0.6	8.3 ± 0.9	2.9 ± 0.5
NO	E_a (eV)	0.55 ± 0.01	0.40 ± 0.03	0.34 ± 0.02
	R^2	0.988	0.965	0.912
	R_p (600°C) (Ω cm^2)	31 ± 1	76 ± 3	48 ± 6
NO_2	E_a (eV)	0.75 ± 0.01	0.88 ± 0.01	0.86 ± 0.01
	R^2	0.996	0.996	0.993
	R_p (600°C) (Ω cm^2)	6.3 ± 0.3	5.7 ± 0.6	2.7 ± 0.1
NO + O_2	E_a (ev)	0.97 ± 0.01	0.86 ± 0.01	0.72 ± 0.11
	R^2	0.999	0.993	0.999
	R_p (600°C) (Ω cm^2)	7.2 ± 0.2	3.6 ± 0.5	2.4

Table II. E_a values together with the corresponding R^2 values for the fit, EC values, R_{MF}, and R_{LF} values at 600°C for MF and LF arcs in 1% NO in Ar with a flow of 100 mL/min.

		LSM15/CGO10	LSM50/CPO10	LSM50/CPO20
MF	E_a (eV)	0.64 ± 0.02 eV	0.67 ± 0.03 eV	0.63 ± 0.05 eV
	R^2	0.990	0.977	0.977
	EC (F cm^{-2})	8×10^{-5} to 5×10^{-3}	3×10^{-4} to 5×10^{-2}	5×10^{-4} to 2×10^{-2}
	R_{MF} (600°C) (Ω cm^2)	6.8 ± 0.5	5.8 ± 0.6	5 ± 0.1
LF	E_a (eV)	0.34 ± 0.02	0.48 ± 0.01	0.46
	R^2	0.980	0.978	0.998
	EC (F cm^{-2})	1×10^{-2} to 1×10^{-1}	2–4 $\times 10^{-1}$	3–7 $\times 10^{-1}$
	R_{LF} (600°C) (Ω cm^2)	6.8 ± 0.5	68 ± 2	42 ± 7

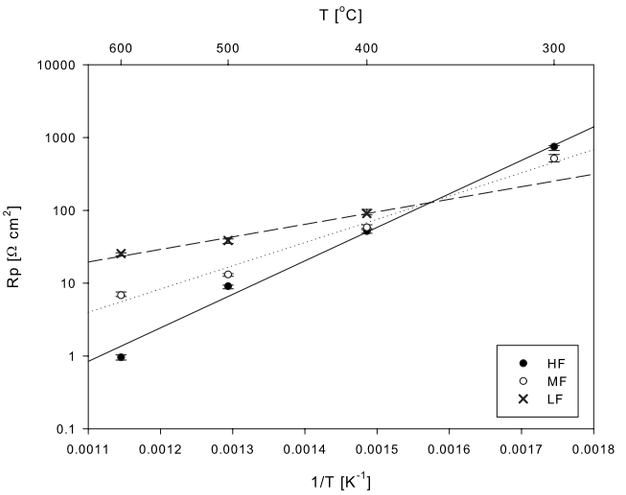

Figure 8. The R_{HF} (●), R_{MF} (○), and R_{LF} (×) for the LSM15/CGO10 electrodes in 1% NO in Ar as a function of the inverse temperature.

increased with increasing flow rate. This phenomenon was observed for both the LSM50/CPO10 and LSM50/CPO20 cells in the temperature range of 400–600°C.

NO_2.— An equilibrium between NO, O_2, and NO_2 may be established according to Eq. 6, and due to fast kinetics at high temperatures, a part of the NO_2 present in the inlet gas stream is converted into O_2 and NO

$$NO_2 \leftrightarrow NO + \tfrac{1}{2}O_2 \qquad [6]$$

The concentration of NO_2 described for the experiments in this section is thus based on the concentration in the inlet gas stream, while the actual concentration around the cell might be different. The Testo 350-S flue gas analyzer was used to measure the ratio between NO and NO_2 in the temperature range 400–600°C to determine exactly how much NO_2 was present. The ratios between NO_2 and NO were 2.7 and 0.9 at 400 and 500°C, respectively, while it was as low as 0.7 at 600°C.

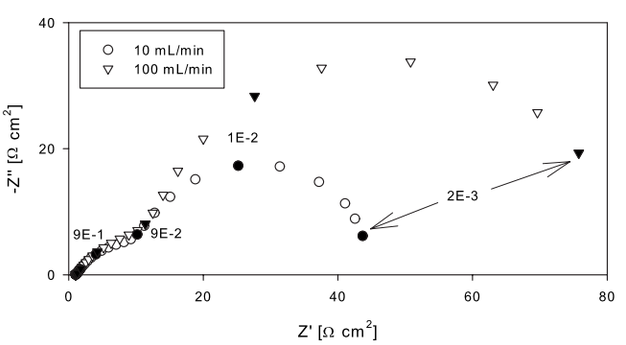

Figure 9. Impedance plots for LSM50/CPO20 cells in 1% NO at 600°C with a gas flow of 10 (○) and 100 mL/min (●). The frequency of the data point is given in hertz for the solid points.

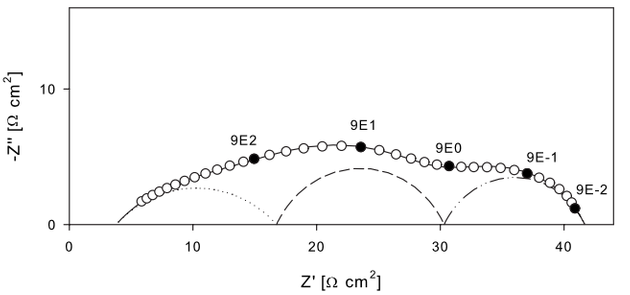

Figure 10. The impedance spectra for LSM15/CGO10 electrodes in 1% NO_2 in Ar at 500°C along with the deconvolution of the data (dotted lines). For the solid points the frequency of the data point is given in hertz.

Three to four arcs were found in the impedance plots for cells in 1% NO_2 in Ar. There were two large arcs, one at MF and one at LF. The resistance of the MF arc decreased more with temperature than the LF arc, and at 400°C, the LF arc could not be seen anymore. When the impedance plots for LSM15/CGO10 electrodes in 1% NO_2 in Ar at 500 and 600°C (Fig. 10 and 7) are compared, the MF arc clearly decreases much more with temperature than the LF arc.

For the electrodes containing CPO, the resistance of the LF arc did not seem to vary with temperature, as it could only be seen in the impedance spectra at 500 and 600°C, and even at 500°C, it was merely a distortion of the spectra in the LF end. The EC for this arc was in the range of 4×10^{-2} to 6×10^{-1} F cm^{-2} for the LSM50/CPO10 and LSM50/CPO20 electrodes. For the LSM15/CGO10 electrodes, an activation energy of 0.58 ± 0.03 eV was calculated for the LF arc with an EC in the range 1–2 $\times 10^{-2}$ F cm^{-2}. But in the LSM15/CGO10 electrodes, there was another arc present at an even lower frequency at 600°C with an EC equal to 1.9 $\times 10^{-2}$ F cm^{-2}. The activation energy for the MF arc for the three types of electrodes together with the corresponding EC range can be seen in Table III.

N_2O.— Only the LSM50/CPO20 electrodes were subjected to EIS in 1% N_2O in Ar at 500 and 600°C. The impedance plot was composed of three arcs. R_p was very large, more than 15 times larger than that for electrodes in 1% NO_2 at 600°C. Changing the gas flow from 100 to 10 mL/min had no effect on the impedance plot or value of R_p.

$NO + O_2$.— The electrodes were subjected to impedance spectroscopy, while 0.75% NO and 5% O_2 were present in the atmosphere. The impedance plots are composed of three to four arcs with one large arc dominating. A smaller LF arc can be found at higher temperatures. The R_p of the electrodes were lower than the R_p of electrodes in 1% NO in Ar in most cases, as seen in Fig. 11 and 12.

Discussion

Matching of arcs to processes.— Several distinct arcs are seen in the impedance plots, and we tried to match these arcs to the

Table III. E_a values together with the corresponding R^2 values for the fit, EC, and R_{MF} values at 600°C values for resistance of MF arc in 1% NO_2 in Ar.

Electrode	E_a (eV)	EC (F cm^{-2})	R_{MF}(600°C) (Ω cm^2)
LSM15/CGO	0.82 ± 0.04 (R^2 = 0.973)	9×10^{-5} to 2×10^{-4}	2.420 ± 0.005
LSM50/CPO10	1.00 ± 0.01 (R^2 = 0.991)	1×10^{-4} to 1×10^{-2}	3.3 ± 0.7
LSM50/CPO20	0.73 ± 0.02 (R^2 = 0.967)	6×10^{-4} to 7×10^{-2}	1.5 ± 0.2

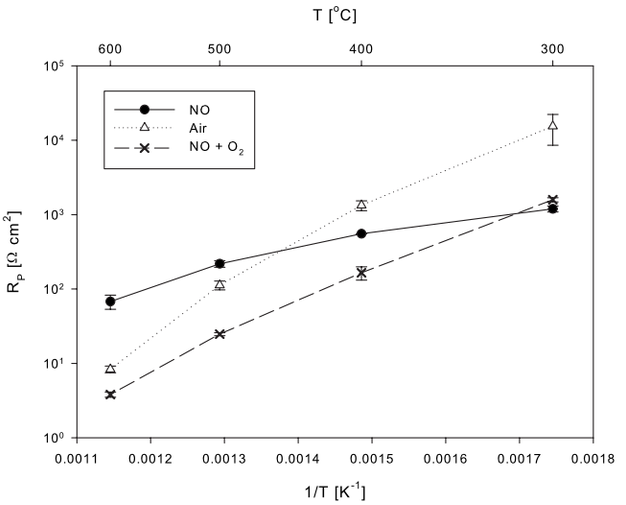

Figure 11. The R_p for the LSM50/CPO10 electrodes in 1% NO in Ar (●), air (△), and 0.75% NO and 5% O_2 in Ar (×) as a function of the inverse temperature.

processes. Some of the arcs described in the Results section are called MF and LF because of their location in the impedance plot, but the EC and summit frequency depend on the temperature. Therefore, it would be more convenient to use another naming system, and we used the same names that Jørgensen and Mogensen used in Ref. 18 where five types of arcs, A–E, were identified.

In the HF area of the impedance plots, one or two small arcs seem to be present for all the impedance plots. They are not affected by the change in atmosphere nor flow, but they do depend on temperature. Typically, the activation energy is around 1 eV, and the arcs are quite depressed with α values around 0.4–0.6. We believe that these arcs are similar to the arcs of types A and B, which cannot always be separated.

These arcs are related to the transport of oxide ions across and through the LSM/doped ceria interface into the dense electrolyte.[18] An MF arc is also identified in many of the impedance arcs. For the spectra recorded in air, the summit frequency of this arc is around 1 Hz for all the tested electrodes at 600°C, which corresponds with

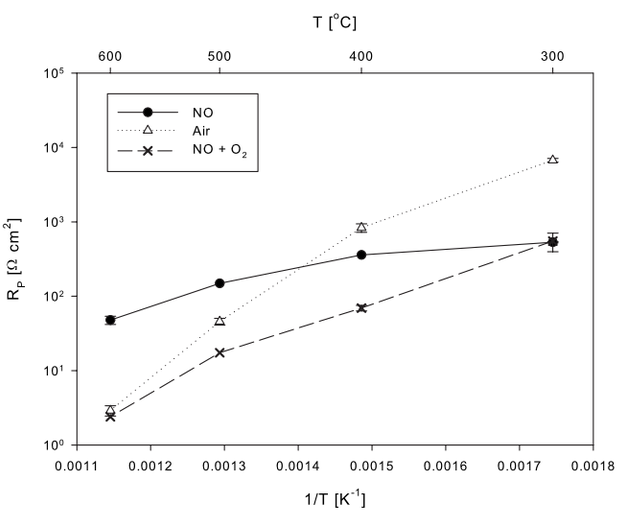

Figure 12. The R_p for the LSM50/CPO20 electrodes in 1% NO in Ar (●), air, and 0.75% NO and 5% O_2 in Ar (×) as a function of the inverse temperature.

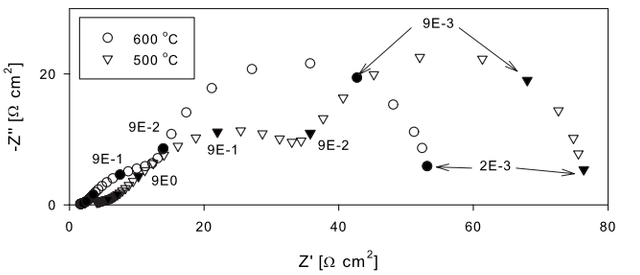

Figure 13. Impedance plots for LSM50/CPO10 electrodes in 1% NO in argon at 500 (▽) and 600°C (○) with a flow of 10 mL/min. For the solid points, the frequency of the data point is given in hertz.

the range given in Ref. 18 for the C arc at 850°C. The processes of arc C are believed to be due to adsorption, surface diffusion, and transfer across the triple phase boundary (TPB). Therefore, the C arc is dependent on the length of the TPB. The activation energy for the C arc in air is around 1.4–1.6 eV for this work, which overlaps with the values reported in Ref. 18 (1.5–2.0 eV). The α value for the MF arc is typically 0.7–0.8 depending on the type of electrode and atmosphere.

When the atmosphere is 1% NO in Ar, the activation energy for the C arc decreases from 0.5 to 0.7 eV, while it is higher for the CPO-containing electrodes in 1% NO_2 in Ar (1.1–1.2 eV).

All the electrodes in the NO-containing atmosphere had a very large LF arc present in the impedance spectra in the temperature range of 400–600°C. Especially for the electrodes containing CPO, the LF arc had a high EC, 2–4 × 10^{-1} and 3–7 × 10^{-1} F cm^{-2} for LSM50/CPO10 and LSM50/CPO20, while LSM15/CGO10 had an EC in the range 1 × 10^{-2} to 1 × 10^{-1} cm^{-2}. The α value was very high, around 0.9–0.98, and in some cases the arc could be fitted with an *RC* element instead of an *RQ* element.

Variation in the flow rate had a large effect on the size of all the LF arcs, and the resistance increased with the flow rate, as illustrated in Fig. 9.

If the 500 and 600°C impedance plots for the LSM50/CPO10 cells in 1% NO in Ar with flow rate of 10 mL/min are compared (see Fig. 13), it can be seen that the LF arc did not increase with decreasing temperature. So, for a flow of 10 mL/min, there is no activation energy, while there is some temperature dependence at a flow rate of 100 mL/min.

An LF arc with a high α value would usually be associated with conversion impedance,[19] but this arc is not a typical conversion arc as the resistance increases with flow rate, which is the opposite of what is expected for a conversion arc. Conversion impedance was seen for a three-electrode cell, where the working and reference electrodes are in separate atmospheres.[19]

The LF arc must somehow be related to the chemical reactions in the NO_x system as it is only seen here. A process that would fit a conversion impedance could be a reaction, which is impeded by lack of a necessary intermediate reactant. When 1% NO is present and when we increase the flow rate, more NO gets into contact with the electrode, so reactions with NO are not hindered by the shortage of reactants.

NO_2 can be formed catalytically from NO by $La_{1-x}Sr_xMnO_3$ (x = 0.05, 0.15, 0.25, 0.35, and 0.5) in the temperature range of 200–500°C.[20] So, a reaction involving NO_2 as one of the reactants limited by the low concentration of NO_2 could be the cause of the LF arc. N_2O is often suggested as an intermediate,[9] but it is not stable at high temperatures;[21] therefore, it is not likely that a reaction with N_2O as the limiting intermediate is causing the LF arc at 500 and 600°C, although it can be present as a short-lived intermediate. R_p is more than 15 times larger for LSM50/CPO20 electrodes in 1%

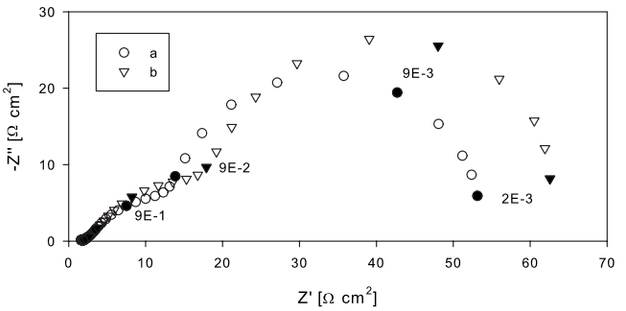

Figure 14. The impedance plots for LSM50/CPO10 electrodes in 1% NO in Ar at 600°C with a flow rate of 10 mL/min. The (a) plot (○) is after 2 h in 1% NO in Ar, while the (b) plot (▽) is after 5 days in 1% NO in Ar.

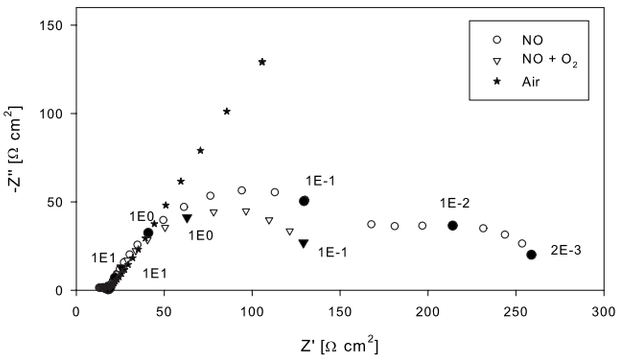

Figure 15. Impedance spectrum for LSM50/CPO20 cells in air (●), 1% NO in Ar (○), and 0.75% NO + 5% O_2 in Ar (▽) at 400°C. For the solid points, the frequency of the data point is given in hertz.

N_2O than in 1% NO_2 in Ar, and also, the R_p of the electrodes in 1% N_2O in Ar does not depend on the gas flow. This supports the idea of NO_2, and not N_2O, as an intermediate.

The hypothesis is that NO_2 is formed catalytically from NO, as described in Eq. 7, where LSM acts as a heterogeneous catalyst; afterward, the electrode reacts electrochemically with NO_2

$$\text{NO} + \text{LSM} \rightarrow \text{NO}_2 + \text{reduced LSM} \quad [7]$$

The LF arc is also seen in the spectra for cells in 1% NO_2 in Ar at 500 and 600°C, but it is much smaller than in the spectra for cells in NO, which corresponds well with the higher concentration of NO_2. Also, the arc does not increase with decreasing temperature for electrodes in NO_2 in Ar, which is expected as the actual concentration of NO_2 increases at lower temperatures.

The impedance plots for cells in an atmosphere of NO and O_2 in Ar also include a small LF arc at 600 and 500°C, and the EC values were in the range of the ones for the large NO LF arc for all the electrodes. Again, some NO_2 must be present due to the equilibrium between NO, O_2, and NO_2.

These results indicate that NO does not directly react electrochemically with the electrode around OCV but only indirectly via the intermediate. If NO reacts electrochemically with the electrodes, then the reaction has a much higher resistance than the reaction proceeding via an intermediate. But if the *R* value of this process is much larger than that of the reaction with the intermediate, then it is not visible in the impedance spectra, as it mainly reflects the path of the equivalent circuit with the lowest overall resistance.

The NO_2 formed is quickly flushed away at the high flow rate, while at the low flow rate, the concentration of NO_2 close to the electrodes is higher. This could explain why the resistance of the LF arc is higher at high flow rates than at low flow rates.

When NO_2 is formed from NO on the perovskite and O_2 is not present in the atmosphere, then the perovskite must slowly become understoichiometric with respect to oxygen (see Eq. 7), and its ability to form NO_2 should decrease in time. This is illustrated in Fig. 14 where the resistance of the LF arc has clearly increased after 5 days in a NO-containing atmosphere. But even after 5 days, the presence of the arc means that NO_2 is still being formed. This suggests that some other species than the perovskite is being reduced, and in this system, the only other candidate would be the formation of N_2O from NO. An equilibrium such as that in Eq. 8 could be formed

$$3\text{NO} \leftrightarrow \text{N}_2\text{O} + \text{NO}_2 \quad [8]$$

O_2 could also be a candidate for the component, which causes the LF conversion arc due to a low concentration in case a small leak was present in the setup. O_2 is not supposed to be present in the 1% NO in Ar atmosphere, as the setup has been leak tested before experiments. But this could explain that R_p increases with flow rate; the higher the flow rate, the less effect a possible leak would have. The LF arc, however, has also been identified in the spectra for electrodes in 0.75% NO + 5% O_2 in Ar, and as there is no lack of O_2 in this atmosphere, a diffusion arc due to lack of O_2 should be unlikely. Furthermore, the size of the LF arc depends quite strongly on the type of LSM–doped ceria composite, which may be explained by significant differences between the heterogeneous catalytic activity for the NO_2 forming processes.

Temperature dependence.— The electrodes had a much lower R_p for 1% NO or NO_2 in Ar than for air in the 300–400°C range. The R_p for the electrodes in air at 600°C was lower than 1% NO in Ar and similar to 1% NO_2 in Ar, but the activation energy for R_p in air was larger than for 1% NO or NO_2 in Ar for nearly all the electrodes examined; the only exception being the LSM50/CPO10 electrodes, which had a larger E_a for 1% NO_2 in Ar than for air.

As the actual temperatures in the exhaust of a diesel engine is in the region of 200–300°C, it is optimal that the electrodes tested have lower resistances for NO_x than for air in the low temperature range.

The apparent E_a for electrodes in 1% NO in Ar was much lower than for air; this is mostly due to the large LF arc dominating the spectra in NO at high temperatures. When the E_a for the MF arc, type C, are compared, the values in air are still higher than that in 1% NO in Ar. Thus, the electrodes react more easily with the intermediate (or NO) at low temperatures than with O_2. This could be due to changes in the kinetics at lower temperature, as the LF arc cannot be identified in the impedance spectra at 300°C for electrodes in 1% NO in Ar. The low pO_2 pressure could also affect the electrodes.

Addition of oxygen.— When 5% O_2 was added to the atmosphere containing 0.75% NO in Ar, the R_p either decreased (high temperatures) or did not increase nearly as much as could be expected when looking at the very high R_p for air in the temperature range of 300–400°C. This can be interpreted as the oxygen did not inhibit the reaction between the electrodes and NO_2. The addition of oxygen decreases the R_p compared to the situation when only NO and Ar are present at some temperatures, as seen in Fig. 15.

The LF arc, which is usually present in the impedance spectra recorded in the atmosphere containing NO, is very small or missing when 5% O_2 is present. The first part of the impedance spectra for LSM electrodes in 1% NO in Ar and in 5% O_2 + 0.75% NO in Ar are similar (see Fig. 15). The lack of the LF arc could be explained by the presence of NO_2 from the reaction between O_2 and NO.

An alternative explanation could be that the electrodes become more efficient at reducing O_2, when NO are present, due to the formation of a more reactive oxygen surface species from the reaction between NO and O_2, as suggested by Reinhardt et al.[2]

Doping with Pr.— The LF arc in NO was larger for the electrodes containing CPO, and the EC was higher compared to the LSM15/CGO10 electrodes, shifting the LF arc to even lower fre-

quencies. The summit frequency of the LF arc at 600°C for CPO-containing electrodes was around 5 mHz, while it was around 250 mHz for the LSM15/CGO10 electrodes. This shift to higher capacitance (Table II) must be related to the doping of ceria with Pr. The Pr ions can change the oxidation state between 3+ and 4+ much easier than Ce and Gd. Thus, the higher capacitance may come from charge storage in the Pr ions. This corresponds well with the LSM50/CPO20 having higher capacitances than the LSM50/CPO10 (see Table II), which contains only half the amount of Pr ions.

The LSM50/CPO20 electrodes generally have lower R_p than the LSM50/CPO10 electrodes regardless of temperature and atmosphere (compare Fig. 11 and 12). The addition of Pr to ceria can increase electronic conductivity, and as CPO20 contains twice as much Pr as CPO10, that could explain the lower R_p values.

The two sets of electrodes that contained CPO10 and CPO20, respectively, had a lower overall apparent E_a in atmospheres containing NO compared to the LSM15/CGO10 electrodes and also had a higher apparent E_a in air than LSM15/CGO10 electrodes (see Table I). Furthermore, the electrodes with the most Pr, LSM50/CPO20, had the lowest E_a in NO and the highest E_a in air. This is due to higher R_{LF} of the CPO-containing electrodes at high temperatures, where R_{LF} dominates the spectra. The LSM50/CPO10 and LSM50/CPO20 electrodes must have less catalytic activity for producing NO_2 compared to the LSM15/CGO10 electrodes at the high temperatures, as the LF arc is linked to the concentration of the intermediate. This can be caused by the CPO doping, but the variation in Sr content between LSM15 and LSM50 might also play a role.

Conclusion

All the impedance data were fitted with equivalent circuits, and between two and four arcs were identified in each impedance spectrum. Changing the atmosphere and temperature had a large impact on the appearance of the impedance spectra and on the size of the R_p. The electrodes were more active in atmospheres containing NO or NO_2 at low temperature, as the R_p was much smaller than that in air. The addition of 5% O_2 lowered the R_p for electrodes in 1% NO in Ar.

The electrodes had a lower apparent E_a in NO_x-containing atmosphere than in air. The electrodes containing CPO had a lower E_a in a NO-containing atmosphere than the LSM15/CGO10 electrodes. Further, the electrodes of type LSM50/CPO20 had the lowest R_p when the atmosphere was 1% NO or NO_2 in Ar at the temperatures of 300–400°C.

The resistance was significantly lower in 1% NO_2 in Ar than for 1% NO in Ar at higher temperatures, mostly due to the large LF arc seen in the NO impedance spectrum for all types of electrodes. The same type of arc was also seen in the spectra for electrodes in NO + O_2 and NO_2. This arc is a type of conversion arc caused by a reaction, which is limited by a low concentration of intermediate reactants. The electrodes seem to be relatively inactive toward NO around OCV when no O_2 or NO_2 is present at high temperatures. The intermediate is probably NO_2, as the electrodes have much lower R_p in an atmosphere containing NO_2. Therefore, the reaction causing the LF arc likely takes place through the following reaction steps: First, the intermediate, NO_2, is formed catalytically from NO by LSM, and then the electrode reacts electrochemically with NO_2.

Acknowledgments

This work was supported financially by The Programme Commission on Sustainable Energy and Environment, The Danish Council for Strategic Research, via the Strategic Electrochemistry Research Center (www.serc.dk) under contract no. 2104-06-0011. Dr. T. Jacobsen of the Technical University of Denmark is acknowledged for his fruitful discussions. P. Jørgensen of Risø National Laboratory for Sustainable Energy, Technical University of Denmark is acknowledged for FIB-SEM imaging of the sample of symmetrical cell.

Technical University of Denmark assisted in meeting the publication costs of this article.

References

1. S. Pancharatnam, R. Huggins, and D. Mason, *J. Electrochem. Soc.*, **122**, 869 (1975).
2. G. Reinhardt, H.-D. Wiemhöfer, and W. Göpel, *Ionics*, **1**, 32 (1995).
3. T. Hibino, *J. Appl. Electrochem.*, **25**, 203 (1994).
4. E. Wachsman, P. Jayaweera, G. Krishnan, and A. Sanjurjo, *Solid State Ionics*, **136–137**, 775 (2000).
5. K. Kammer, *Appl. Catal., B*, **58**, 33 (2005).
6. T. Hibino, K. Ushiki, and Y. Kuwahara, *Solid State Ionics*, **98**, 185 (1997).
7. Y. Teraoka, T. Harada, and S. Kagawa, *J. Chem. Soc., Faraday Trans.*, **94**, 1887 (1998).
8. C. Tofan, D. Klvana, and J. Kirchnerova, *Appl. Catal., A.*, **223**, 275 (2002).
9. T. Ishihara, M. Ando, K. Sada, K. Takiishi, K. Yamada, H. Nishiguchi, and Y. Takita, *J. Catal.*, **220**, 104 (2003).
10. L. Woo, L. Martin, R. Glass, and R. Gorte, *J. Electrochem. Soc.*, **154**, J129 (2007).
11. M. Stranzenbach and B. Saruhan, *Sens. Actuators B*, **137**, 154 (2009).
12. T. Hibino, Y. Kuwahara, T. Otsuka, N. Ishida, and T. Oshima, *Solid State Ionics*, **107**, 213 (1998).
13. T. Hibino, Y. Kuwahara, T. Otsuka, N. Ishida, and T. Oshima, *Solid State Ionics*, **107**, 217 (1998).
14. L. Chick, L. R. Pederson, G. D. Maupin, J. L. Bates, L. E. Thomas, and G. J. Exarhos, *Mater. Lett.*, **10**, 6 (1990).
15. E. Barsoukov and J. MacDonald, *Impedance Spectroscopy: Theory, Experimental, and Applications*, 2nd ed., p. 37, Wiley Interscience, New York (2005).
16. T. Jacobsen, B. Zachau-Christensen, L. Bay, and S. Skaarup, in *Proceedings of the 17th Risø International Symposium on Materials Science*, F. W. Poulsen, N. Bonanas, S. Linderoth, M. Mogensen, and B. Zachau-Christensen, Editors, Risø National Laboratory, p. 29 (1996).
17. B. Boukamp, *Solid State Ionics*, **20**, 31 (1986).
18. M. Jørgensen and M. Mogensen, *J. Electrochem. Soc.*, **148**, A433 (2001).
19. S. Primdahl and M. Mogensen, *J. Electrochem. Soc.*, **145**, 2431 (1998).
20. K. K. Hansen, E. Skou, H. Christensen, and T. Turek, *J. Catal.*, **199**, 132 (2001).
21. P. Kofstad, *Uorganisk Kjemi*, 2nd ed., p. 210, TANO, Oslo (1987).